AIAA JOURNAL
Vol. 44, No. 7, July 2006

Stability Analysis of Stitched Composite Plate System with Delamination Under Hygrothermal Pressure

A. Kadir Yavuz,* Katerina D. Papoulia,† S. Leigh Phoenix,‡ and C. Yuen Hui‡
Cornell University, Ithaca, New York 14853

A stitched composite structure made of fiber-reinforced polymers is analyzed. This composite structure is modeled by two specially orthotropic adhesively bonded, delaminated and stitched plates under in-plane compressive and shear loads and internal hygrothermal pressure acting on delamination surfaces of the two plates, which are considered as identical, and simply supported. Whereas the adhesive layer between plate layers is modeled by mechanical linear normal and shear springs, stitches are modeled by discrete bilinear normal springs for the first time in the literature. In the stitches modeling, it is assumed that they can carry only normal loads because they are very thin and also initial imperfections are included with the parameter of looseness because the stitching yarns are slack initially. The mathematical model of the problem is solved by Rayleigh–Ritz method. After the strain energies of plates, the adhesive layer and the stitches and energy potentials for external loads such as compressive normal loads, shear loads, and internal hygrothermal pressure are expressed, sine series as shape functions for plate vertical deflections satisfying simply supported boundary conditions are applied. Then, minimizing the total energy gives deflections for the given loading. The stability condition is obtained as an eigenvalue problem to give critical buckling loads and corresponding mode shapes as well. Results are presented as plots of deformed shapes of the system and tables of parametric studies showing effects of changing parameters on stitch stresses and displacements, critical buckling loads, and corresponding mode shapes.

Nomenclature

a	=	length of plate layers
b	=	width of plate layers
C_i	=	weighting coefficients of vertical deflections' approximation functions, $i = 1, 2$
D_{ij}	=	bending stiffnesses of plate layers, $i, j = 1, 2, 6$
E^a	=	Young modulus of the adhesive layer
E^{st}	=	Young modulus of stitch wires
G^a	=	shear modulus of the adhesive layer
h	=	thickness of plate layers
h^a	=	thickness of the adhesive layer
m_0	=	number of sine terms in x direction in the double Fourier sine series
N_{0x}	=	external compressive normal loads in x direction
N_{0xy}	=	external shear load
N_{0y}	=	external compressive normal loads in y direction
n_d	=	number of delamination holes in the adhesive layer
n_s	=	number of stitches
n_0	=	number of sine terms in y direction in the double Fourier sine series
p_0	=	internal hygrothermal pressure in delaminations
w_i	=	vertical deflections of plate layers, $i = 1, 2$
δ_0	=	looseness parameter of initially slack stitch wires

Presented as Paper 2005-2106 at the AIAA/ASME/ASCE/AHS/ASC 46th Structures, Structural Dynamics, and Materials Conference, AIAA/ASME/AHS 13th Adaptive Structures Conference, AIAA 7th Non-Deterministic Approaches Forum, AIAA 6th Gossamer Spacecraft Forum, and AIAA 1st Multidisciplinary Design Optimization Specialist Conference, Austin, TX, 18–21 April 2005; received 25 April 2005; revision received 17 January 2006; accepted for publication 22 January 2006.

*Research Associate, Theoretical and Applied Mechanics, 111 Thurston Hall. Member AIAA.
†Assistant Professor, School of Civil and Environmental Engineering, 363 Hollister Hall.
‡Professor, Theoretical and Applied Mechanics, 321 Thurston Hall.

I. Introduction

FIBER-REINFORCED polymers (FRP) have been very popular composite materials in the aerospace industry for about 40 years. Their most important properties are having high strength-to-weight ratio, adjustable thermomechanical properties, and fatigue resistance. Depending on the application, FRP may carry impact loading, axial compressive loading, shear loading, and hygrothermal loading, which may cause delamination in between laminates by debonding them. Existence of internal pressure in delamination created by hygrothermal effects will cause this failure to propagate rapidly to reduce the effective moment of inertia of the FRP structure. Besides, if the size and/or location of delamination becomes critical, then the debonded layers can even buckle.[1] In other words, delamination changes the stability characteristics of the structure. Therefore, it must be prevented, or at least its propagation must be stopped if there is one.

Researchers believe that stitching is the most effective solution to this failure.[2] By stitching, you put fibers through the thickness of the laminated composite material to increase through-the-thickness shear strength.[3] Kevlar® and shape memory alloys have been used for stitching.[4] However, stitching may reduce the structure's mechanical performance as stitches get closer together. Therefore, to determine an optimum stitching technique is very crucial. A very recent work of the present authors is the first stability analysis considering both delamination and stitching effects in a FRP-based composite structure under only compressive normal loads and hygrothermal pressure (HTP) by assuming perfect stitching.[5]

In this paper, this composite structure is modeled by two specially orthotropic adhesively bonded, delaminated and stitched plates with simply supported boundary conditions (SSBCs) under in-plane compressive and shear loads (defined per unit length) and HTP (defined per unit area) acting on delamination surfaces of plates (Fig. 1). The adhesive interlaminar layer is modeled by continuous mechanical normal and shear springs because they can carry both normal and shear loads.[5–7] However, the stitch wires can carry only normal loads and may be loose because of initial imperfections in stitching. Therefore, they are modeled by discrete bilinear normal springs for the first time in the literature. (In the present paper, the term bilinear means piecewise linear in two regions.) Furthermore, this analysis can handle any combination of circular, elliptical, and rectangular delaminations.

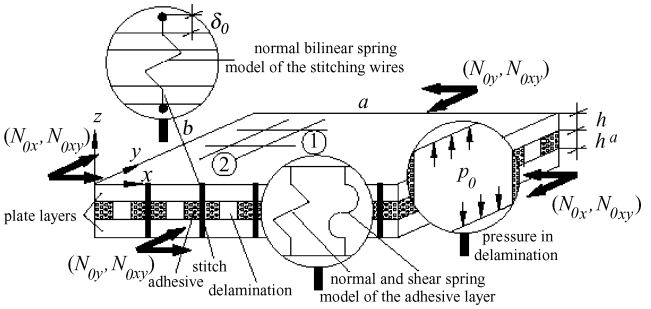

Fig. 1 General system configuration.

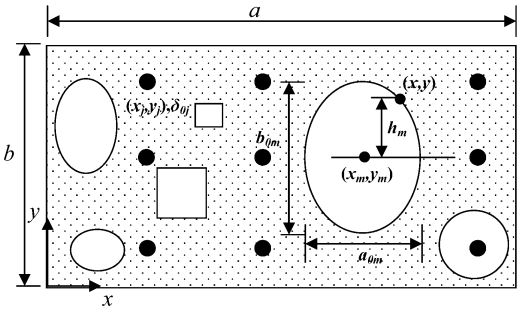

Fig. 2 Center locations of delaminations (x_m, y_m) and stitches (x_j, y_j).

To solve the problem for both deformed shapes and critical buckling loads, the Rayleigh–Ritz method which is very useful for plate problems is applied. First, strain energies of plates, the adhesive layer and stitches, and energy potentials for external loads such as compressive normal loads, shear loads, and HTP are expressed. Then, sine series, which are taken as shape functions for plate vertical deflections satisfying SSBCs are applied to all energy expressions. After minimization of total potential energy, an algebraic equation system is obtained for vertical deflections for the given loading, including axial compressive loads, shear loads, and internal HTP. This equation system also gives the stability condition for the system as an eigenvalue problem to give critical buckling load configurations of external normal and shear loads and corresponding mode shapes.

Results are presented as deformed shapes of the system and parametric studies to show effects of changing parameters on critical buckling loads and corresponding buckling modes.

II. Solution Procedure

The Rayleigh–Ritz method is applied to solve the problem because it is very useful for plates with SSBCs (see Refs. 8 and 9). The thin-plate theory with large deflections is used. [Plates are assumed thin as long as side-to-thickness ratio (a/h) is bigger than 20 (Ref. 9).] In the stability analysis, membrane stresses are generally taken constant and equal to corresponding external compressive stresses.[5–10] In the application of the method, first, potential energy expressions for each component of the system are written. Then, the total potential energy of the system is minimized with respect to each unknown weighting coefficient of approximation functions of vertical deflections (which are sine series to satisfy SSBCs automatically) to obtain the algebraic equation system.

A. Potential Energy Expressions of System Components

Total potential energy of the plate layers, the external compressive normal and shear loads, and the interlaminar adhesive layer (Fig. 1) is given by[5–10]

$$U_0 = \frac{1}{2}\int_0^a \int_0^b \left\{ \sum_{i=1}^{2} \left[D_{11}^{(i)} \left(\frac{\partial^2 w_i}{\partial x^2} \right)^2 + 2D_{12}^{(i)} \frac{\partial^2 w_i}{\partial x^2} \frac{\partial^2 w_i}{\partial y^2} + D_{22}^{(i)} \left(\frac{\partial^2 w_i}{\partial y^2} \right)^2 + 4D_{66}^{(i)} \left(\frac{\partial^2 w_i}{\partial x \partial y} \right)^2 - N_{0x} \left(\frac{\partial w_i}{\partial x} \right)^2 - N_{0y} \left(\frac{\partial w_i}{\partial y} \right)^2 - 2N_{0xy} \left(\frac{\partial w_i}{\partial x} \frac{\partial w_i}{\partial y} \right)^2 \right] + k^n (w_2 - w_1)^2 + k^s \frac{h^2}{4} \left[\left(\frac{\partial w_1}{\partial x} + \frac{\partial w_2}{\partial x} \right)^2 + \left(\frac{\partial w_1}{\partial y} + \frac{\partial w_2}{\partial y} \right)^2 \right] \right\} \mathrm{d}x\, \mathrm{d}y \quad (1)$$

Total potential energy of delaminated parts (Fig. 2) with HTP of the adhesive layer is

$$U_d = \sum_{m=1}^{n_d} \int_{x_m - a_{0m}/2}^{x_m + a_{0m}/2} \int_{y_m - h_m}^{y_m + h_m} \frac{1}{2} \left\{ k^n (w_2 - w_1)^2 + k^s \frac{h^2}{4} \left[\left(\frac{\partial w_1}{\partial x} + \frac{\partial w_2}{\partial x} \right)^2 + \left(\frac{\partial w_1}{\partial y} + \frac{\partial w_2}{\partial y} \right)^2 \right] - 2p_{0m}(w_1 - w_2) \right\} \mathrm{d}x\, \mathrm{d}y \quad (2)$$

where $\boldsymbol{a}_0$ and $\boldsymbol{b}_0$ are characteristic dimensions of delamination shapes and

$$h_m = \begin{cases} (b_{0m}/a_{0m}) \sqrt{a_{0m}^2/4 - (x - x_m)^2}, & \text{if it is an ellipse} \\ b_{0m}/2, & \text{if it is a rectangle} \end{cases}$$

$$k^n = E^a/h^a, \qquad k^s = G^a/h^a \quad (3)$$

It is obvious that for circular delaminations $\boldsymbol{a}_0 = \boldsymbol{b}_0$.

Total potential energy of stitches including looseness parameters as initial imperfections becomes

$$U_{\mathrm{st}} = \frac{1}{2} \sum_{j=1}^{n_s} k_j^{\mathrm{st}} (w_{1j} - w_{2j} - \delta_{0j})^2 \quad (4)$$

where the equivalent bilinear normal spring constants of stitch wires are

$$k_j^{\mathrm{st}} = \begin{cases} E^{\mathrm{st}} A^{\mathrm{st}} / (2h + h^a + \delta_{0j}), & \text{if } w_{1j} - w_{2j} > \delta_{0j} \\ 0, & \text{if } w_{1j} - w_{2j} \le \delta_{0j} \end{cases} \quad (5)$$

B. Minimization of Total Potential Energy of the Whole System

The total potential energy of the whole system, then, can be expressed as follows:

$$\Pi = U_0 - U_d + U_{\mathrm{st}} \quad (6)$$

As vertical deflection approximation functions satisfying SSBCs, a double Fourier sine series is chosen in the following form:

$$w_i = \sum_{K=1}^{m_0} \sum_{L=1}^{n_0} C_{iKL} \sin\left(\frac{K\pi x}{a} \right) \sin\left(\frac{L\pi y}{b} \right) \qquad (i = 1, 2) \quad (7)$$

After substitution of Eq. (7) into Eq. (6), the minimization of total potential requires

$$\frac{\partial \Pi}{\partial C_{1KL}} = 0, \qquad \frac{\partial \Pi}{\partial C_{2KL}} = 0$$
$$(K = 1, 2, \ldots, m_0), \qquad (L = 1, 2, \ldots, n_0) \quad (8)$$

This gives the following algebraic equation system for the unknown weighting coefficients of vertical deflection approximation functions in Eq. (7):

$$\begin{bmatrix}[A1] & [A0]\\ [A0] & [A2]\end{bmatrix}\begin{Bmatrix}\{W1\}\\ \{W2\}\end{Bmatrix}=\begin{Bmatrix}\{P\}\\ -\{P\}\end{Bmatrix}$$

$$\Rightarrow\begin{Bmatrix}\{W1\}\\ \{W2\}\end{Bmatrix}=\begin{bmatrix}[A1] & [A0]\\ [A0] & [A2]\end{bmatrix}^{-1}\begin{Bmatrix}\{P\}\\ -\{P\}\end{Bmatrix} \tag{9}$$

Substitution of this into Eq. (7) gives the deformed shape of the sytem under given loading configuration. If the square matrix including $[\boldsymbol{A0}]$, $[\boldsymbol{A1}]$, and $[\boldsymbol{A2}]$ matrices is singular, then the system is unstable and critical buckling load configurations are obtained from the following eigenvalue problem (EVP) to be solved for any $\boldsymbol{\lambda}$ and $\boldsymbol{\eta}$ combinations as eigenvalues and corresponding buckling mode shapes:

$$\begin{vmatrix}[A1] & [A0]\\ [A0] & [A2]\end{vmatrix}=0 \tag{10}$$

where

$$A1_{IJ}=\left(B_J^{(1)}-\lambda_J+k_0^n+k_{0J}^s\right)\delta_{IJ}-\eta_{IJ}-I_{IJ}^n+S_{IJ}^n-I_{IJ}^s$$

$$A0_{IJ}=\left(-k_0^n+k_{0J}^s\right)\delta_{IJ}+I_{IJ}^n-S_{IJ}^n-I_{IJ}^s$$

$$A2_{IJ}=\left(B_J^{(2)}-\lambda_J+k_0^n+k_{0J}^s\right)\delta_{IJ}-\eta_{IJ}-I_{IJ}^n+S_{IJ}^n-I_{IJ}^s$$

$$W1_{I1}=C_{1I},\qquad W2_{I1}=C_{2I},\qquad P_{I1}=I_I^p+S_I^\delta$$

$$I=(K-1)n_0+L,\qquad J=(M-1)n_0+N$$

$$\delta_{IJ}=\begin{cases}1, & \text{if } I=J\\ 0, & \text{if } I\neq J\end{cases} \tag{11}$$

for Kronecker delta δ. Other parameters in these matrices are

$$B_{KL}^{(i)}=\frac{\pi^4 ab}{4}\left[\frac{D_{11}^{(i)}}{a^4}K^4+\frac{2\left(D_{12}^{(i)}+2D_{66}^{(i)}\right)}{a^2b^2}K^2L^2+\frac{D_{22}^{(i)}}{b^4}L^4\right]$$

$$\lambda_{KL}=\frac{\pi^2 ab}{4}\left(\frac{N_{0x}}{a^2}K^2+\frac{N_{0y}}{b^2}L^2\right)$$

$$\eta_{KLMN}=$$

$$\begin{cases}\dfrac{8KLMN}{(M^2-K^2)(L^2-N^2)}N_{0xy}, & \text{for } M\pm K \text{ odd and } L\pm N \text{ odd}\\ 0, & \text{for } M\pm K \text{ even and } L\pm N \text{ even}\end{cases}$$

$$k_0^n=\frac{ab}{4}k^n,\qquad k_{0KL}^s=\frac{\pi^2h^2ab}{16}\left(\frac{K^2}{a^2}+\frac{L^2}{b^2}\right)k^s$$

$$I_{KLMN}^n=k^n\sum_{m=1}^{n_d}\int_{x_m-a_{0m}/2}^{x_m+a_{0m}/2}\int_{y_m-h_m}^{y_m+h_m}\sin\left(\frac{K\pi x}{a}\right)\sin\left(\frac{L\pi y}{b}\right)\times\sin\left(\frac{M\pi x}{a}\right)\sin\left(\frac{N\pi y}{b}\right)\mathrm{d}x\,\mathrm{d}y$$

$$I_{KLMN}^s=\frac{\pi^2h^2k^s}{4}\sum_{m=1}^{n_d}\int_{x_m-a_{0m}/2}^{x_m+a_{0m}/2}\int_{y_m-h_m}^{y_m+h_m}\left[\frac{KM}{a^2}\cos\left(\frac{K\pi x}{a}\right)\times\sin\left(\frac{L\pi y}{b}\right)\cos\left(\frac{M\pi x}{a}\right)\sin\left(\frac{N\pi y}{b}\right)+\frac{LN}{b^2}\sin\left(\frac{K\pi x}{a}\right)\times\cos\left(\frac{L\pi y}{b}\right)\sin\left(\frac{M\pi x}{a}\right)\cos\left(\frac{N\pi y}{b}\right)\right]\mathrm{d}x\,\mathrm{d}y$$

$$I_{KL}^p=\sum_{m=1}^{n_d}p_{0m}\int_{x_m-a_{0m}/2}^{x_m+a_{0m}/2}\int_{y_m-h_m}^{y_m+h_m}\sin\left(\frac{K\pi x}{a}\right)\sin\left(\frac{L\pi y}{b}\right)\mathrm{d}x\,\mathrm{d}y$$

$$S_{KLMN}^n=\sum_{m=1}^{n_s}k_j^{\mathrm{st}}\sin\left(\frac{K\pi x_j}{a}\right)\sin\left(\frac{L\pi y_j}{b}\right)\times\sin\left(\frac{M\pi x_j}{a}\right)\sin\left(\frac{N\pi y_j}{b}\right)$$

$$S_{KL}^\delta=\sum_{m=1}^{n_s}k_j^{\mathrm{st}}\delta_{0j}\sin\left(\frac{K\pi x_j}{a}\right)\sin\left(\frac{L\pi y_j}{b}\right) \tag{12}$$

III. Results and Discussion

Results are obtained for the following nominal values unless otherwise posted. The plate properties (graphite polyimide) are $a=b=200$ mm, $h=4$ mm, $E=68.95$ GPa, and $G=25.92$ GPa. The adhesive properties (polyimide) are $E^a=2$ GPa, $G^a=0.7$ GPa, and $h^a=2$ mm. The HTP in delaminations is $p_0=6$ MPa. The stitch properties (Kevlar-49) are $E^{\mathrm{st}}=130$ GPa, $d^{\mathrm{st}}=0.357$ mm (diameter), $l^{\mathrm{st}}=4+4+2=10$ mm (characteristic length), tensile strength 3.6 GPa, and corresponding maximum allowable displacement = 0.2769 mm.

First, two examples of the biaxial loading are presented to show how locations of stitch wires and delaminations affect the whole system (Figs. 3a and 4a). In the first one, the configuration has five circular delaminations with nine stitches. The second one has two elliptical delaminations with six stitches. Then, stability of the system under the shear loading is analyzed with the verification of the method for isotropic and specially orthotropic plates.

A. Biaxial Compressive Normal Loading

1. Five Circular Delaminations with Nine Stitch Wires

In this configuration (Fig. 3a), one circular delamination is located at center $(a/2, a/2)$ and four delaminations are located at midcorner points $(a/4, a/4)$, $(a/4, 3a/4)$, $(3a/4, a/4)$, and $(3a/4, 3a/4)$ with $r=a/8$. One center stitch is located at $(a/2, a/2)$; four corner stitches are located at $(a/4, a/4)$, $(a/4, 3a/4)$, $(3a/4, a/4)$, and $(3a/4, 3a/4)$; and four midside stitches are located at $(a/4, a/2)$, $(a/2, a/4)$, $(a/2, 3a/4)$, and $(3a/4, a/2)$.

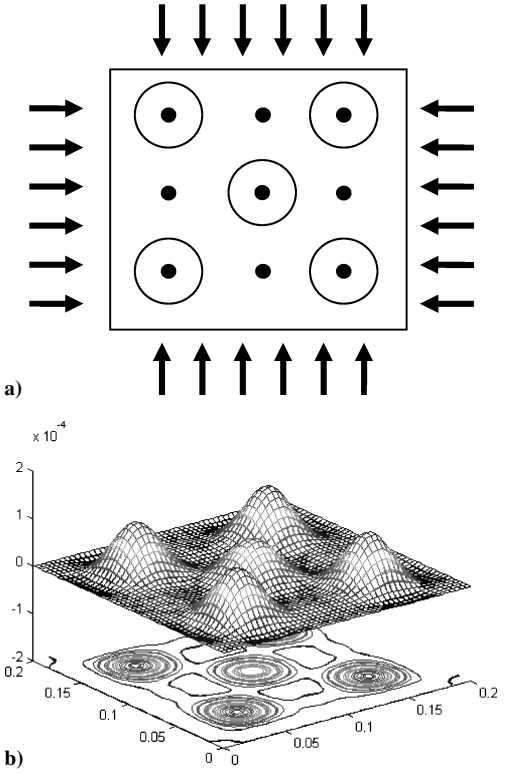

Fig. 3 Sample problem 1: a) configuration for five circular delaminations with nine stitches and b) deformed shape (upper plate).

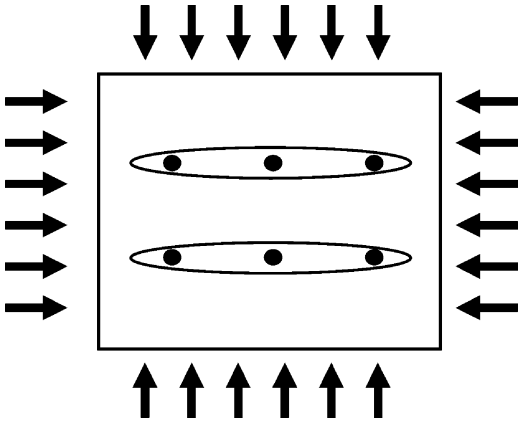

a)

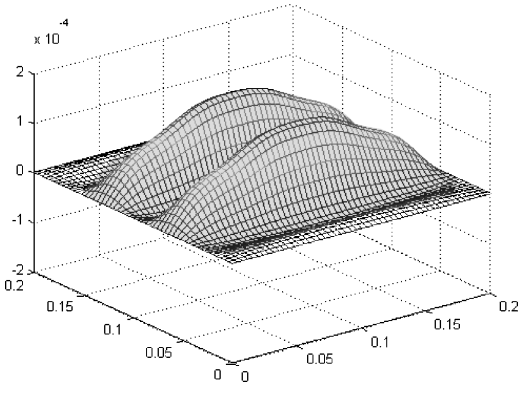

b)

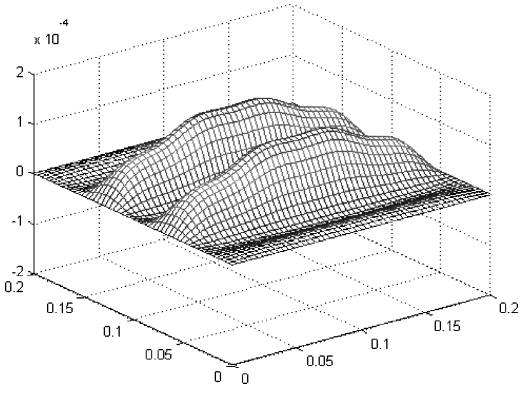

c)

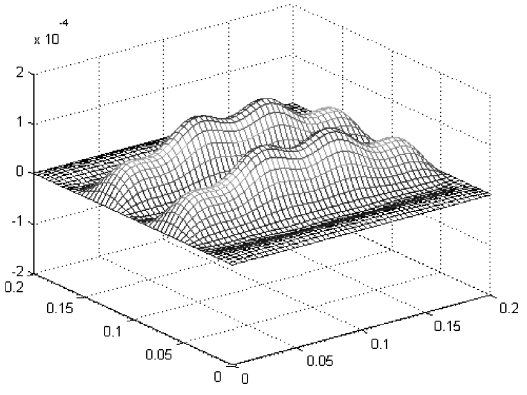

d)

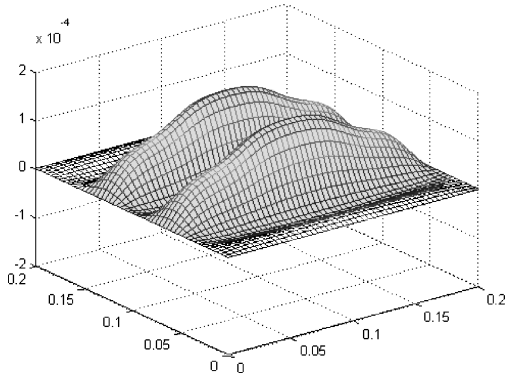

e)

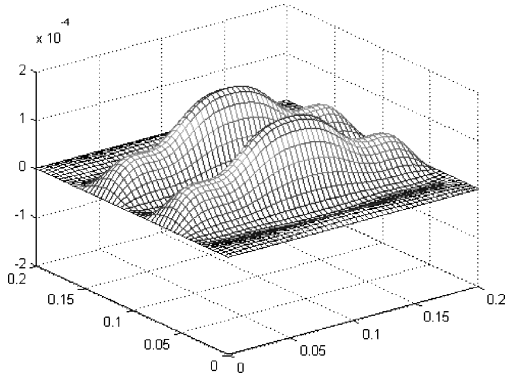

f)

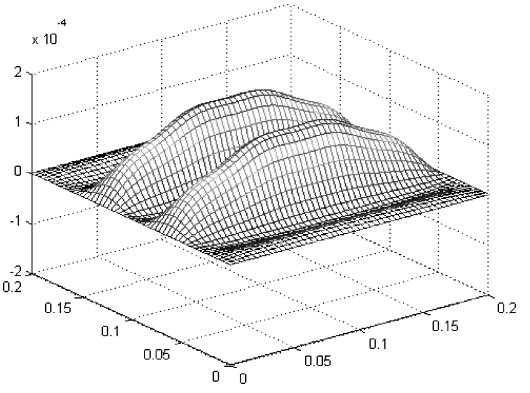

g)

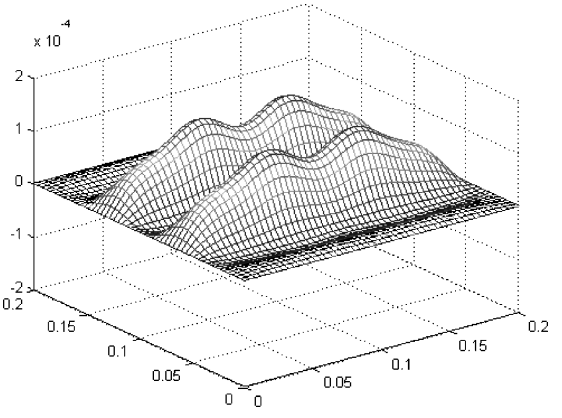

h)

Fig. 4 Sample problem 2: a) configuration for two elliptic delaminations with six stitches (four at sides and two at centers) and deformed shapes (upper plate) for b) no stitch; c) six stitches, $d^{st} = 0.357$ mm; d) six stitches, $d^{st} = 1$ mm; e) four stitches at sides, $d^{st} = 0.357$ mm; f) four stitches at sides, $d^{st} = 1$ mm; g) two stitches at centers, $d^{st} = 0.357$ mm; and h) two stitches at centers, $d^{st} = 1$ mm.

Table 1 Stitch stresses and stretching displacements, $p_0 = 6$ MPa

	Center		Corner		Midside	
N_0, MPa	Stress, GPa	Displacement, mm	Stress, GPa	Displacement, mm	Stress, GPa	Displacement, mm
0	1.6082	0.1237	1.9058	0.1466	−0.0961	−0.0074
0 (no stitch)	——	0.1269	——	0.1512	——	−0.0076
5	2.0314	0.1563	2.5854	0.1989	−0.1102	−0.0085
5 ($d^{st} = 1$ mm)	1.6661	0.1282	2.0134	0.1549	−0.0934	−0.0072
5 (no stitch)	——	0.1614	——	0.2075	——	−0.0087

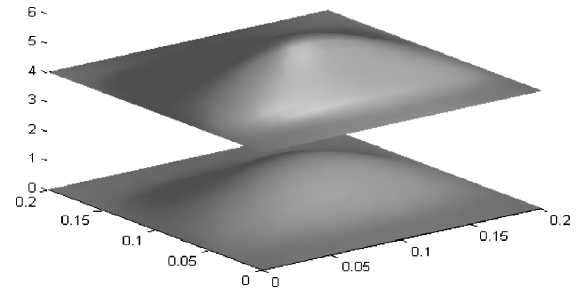

a) Mode 1, $N_{0cr} = 1.39$ MPa

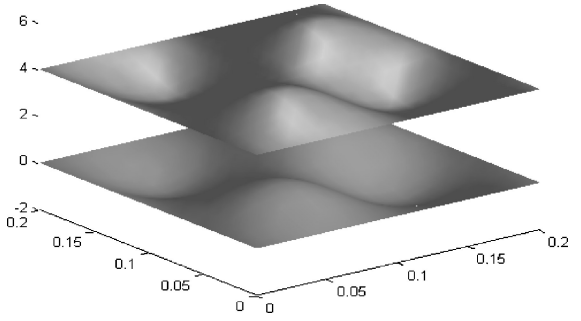

e) Mode 5, $N_{0cr} = 2.49$ MPa

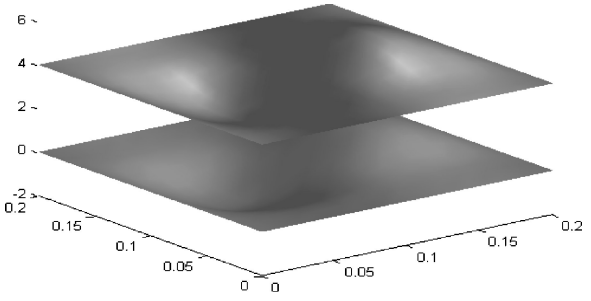

b) Mode 2, $N_{0cr} = 1.81$ MPa

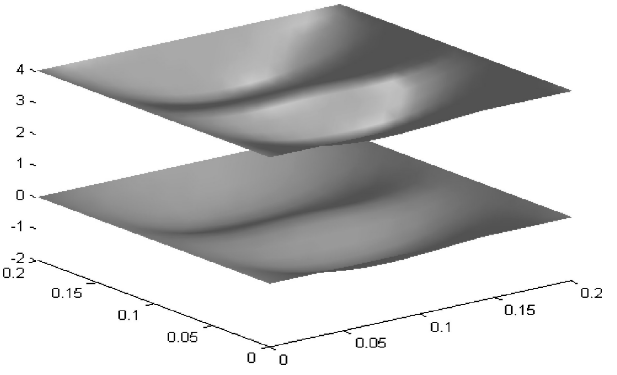

f) Mode 6, $N_{0cr} = 2.65$ MPa

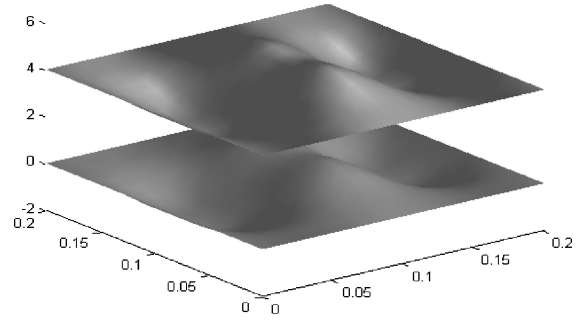

c) Mode 3, $N_{0cr} = 2.26$ MPa

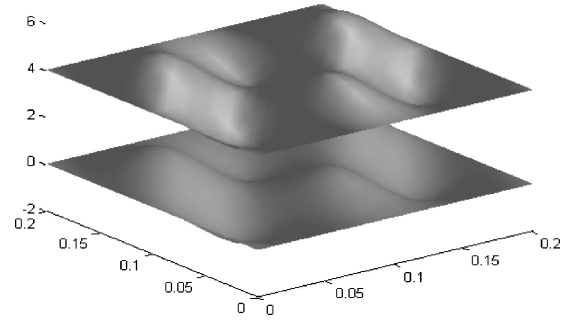

g) Mode 7, $N_{0cr} = 2.77$ MPa

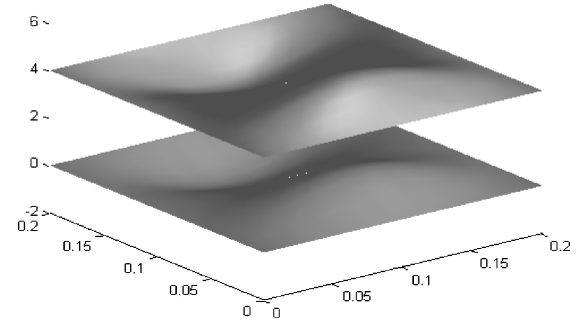

d) Mode 4, $N_{0cr} = 2.41$ MPa

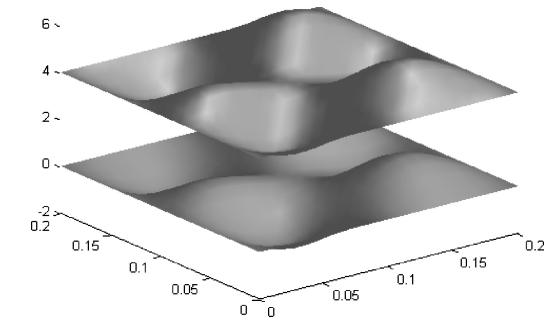

h) Mode 8, $N_{0cr} = 2.80$ MPa

Fig. 5 Buckling mode shapes and corresponding critical buckling loads for configuration of two elliptic delaminations with two center stitches.

The deformed configuration (Fig. 3b) is obtained for $N_{0x} = N_{0y} = N_0 = 5$ MPa. Displacements and stresses of stitch wires are tabulated in Table 1. The last row is obtained for much stiffer stitch wires ($d^{st} = 1$ mm). Because the adhesive is strong, midside stitches are not necessary. Stitches should be placed at possible damage zones to prevent damages from starting or growing. Instead of increasing the number of stitches, the stiffness of stitch should be increased to reduce the damage caused by the stitching process.

2. Two Elliptic Delaminations with Six Stitch Wires

In this example (Fig. 4a), dimensions of elliptic delaminations are $(a_0)_{1,2} = 3a/4$ and $(b_0)_{1,2} = a/10$ and their centers, $(a/2, a/3)$ and $(a/2, 2a/3)$; stitch locations, two at centers and four at sides $(a/4, a/3)$, $(a/4, 2a/3)$, $(3a/4, a/3)$, and $(3a/4, 2a/3)$. Results are shown in Table 2.

The deformed configurations are plotted in Figs. 4b–4h for different stitch patterns such as six stitches, four stitches at sides and two stitches at centers ($N_{0x} = N_{0y} = N_0 = 2$ MPa and $d^{st} = 1$ mm). First eight buckling modes are presented for the two center stitch case and corresponding critical buckling loads (N_{0cr}) are between 1.39 and 2.80 MPa (Fig. 5), which are very close to each other. Stresses and displacements of each stitch wire are tabulated in Table 2 and 3, respectively. The last three rows are obtained for much stiffer stitch wires, $d^{st} = 1$ mm. In the last two rows of Table 2 and 3, because the stitches are slack initially ($\delta_0 = 0.1$ and 1 mm), stitch stresses and stretching displacements go down to zero. Stiffer stitches reduces the displacements drastically. If they are at the right places (here, at centers), two stitches does the job of six stitches.

B. Shear Loading

The effciency of the method in the shear buckling case is shown with weak connection, $E^a = 1.0$ Pa and $G^a = 1.0$ Pa, to give one plate solutions in terms of shear buckling coefficients given by

$$k_0 = b^2(N_{0xy})_{cr}/\pi^2 D, \qquad \gamma_0 = a^2(N_{0xy_{cr}})/\pi^2 D_{22} \qquad (13)$$

for isotropic and specially orthotropic plates, respectively. In Table 4, one can easily see that the aspect ratio plays a big role on the accuracy of the method with the same number of terms. That is why the number of terms must be balanced in both directions for higher aspect ratios.

The method works well for specially orthotropic plates as well. Shear buckling coefficients for this case are presented in Table 5 with different number of terms. Five terms in each direction seem sufficient to obtain reasonable results. To show how the delamination size effects the critical shear buckling load, one center delamination with different radii is considered and related results are presented in Table 6. Two shear buckling modes are presented in Fig. 6 ($r_d/a = 3/8$). Calculated shear buckling coefficients do not seem affected very much by the delamination size in the nominal adhesive layer and with the existence of the adhesive layer.

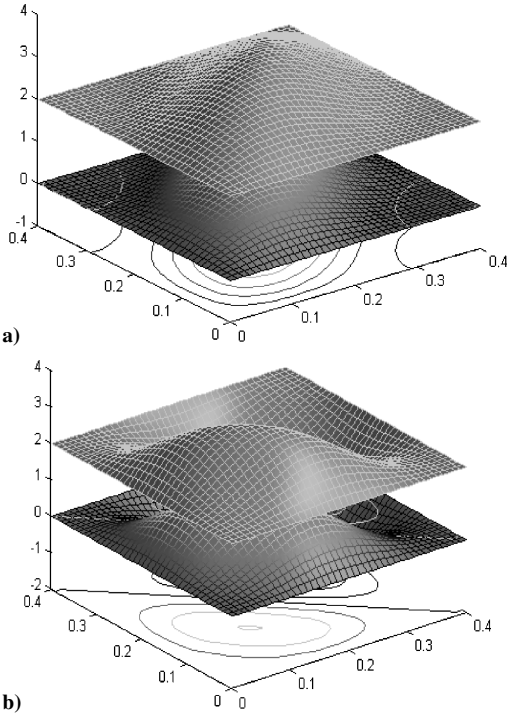

Fig. 6 Shear buckling mode shapes of a) mode 1 and b) mode 2.

Table 2 Stitch stresses, $p_0 = 6$ MPa

	Center, GPa		Sides, GPa	
N_0, MPa	Six stitches	Two stitches	Six stitches	Four stitches
0	3.2157	3.2065	2.3983	2.3921
1	3.4488	3.4362	2.5346	2.5260
2	3.7206[a]	3.7034[a]	2.6874	2.6753
2 ($d^{st} = 1$ mm)	2.6550	2.5826	2.0552	2.0042
2 ($\delta_0 = 0.1$ mm)	1.3501	1.2788	0.7532	1.0090
2 ($\delta_0 = 1$ mm)	0.0	0.0	0.0	0.0

[a]Stitch failure.

Table 4 Shear buckling coefficients k_0 of isotropic rectangular plates for different aspect ratios

	k_0	
a/b	Present	Bulson[10]
1	9.3426	9.3400
2	6.5607	6.3400
3	5.8627	5.7844
4	5.6647	5.5900
5	5.7118	5.5000

Table 5 Shear buckling coefficients γ_0 of specially orthotropic square plates for different number of terms

	γ_0	
$m_0 = n_0$	Present	Whitney[8]
2	392.86	392.9
3	313.68	313.7
4	310.19	310.2
5	308.99	309.0

Table 3 Stitch stretching displacements, $p_0 = 6$ MPa

	Center, mm			Sides, mm		
N_0, MPa	Six stitches	Two stitches	No stitches	Six stitches	Four stitches	No stitches
0	0.2474	0.2467	0.2603	0.1845	0.1840	0.1921
1	0.2653	0.2643	0.2804	0.1950	0.1943	0.2035
2	0.2862[a]	0.2849[a]	0.3042	0.2067	0.2058	0.2164
2 ($d^{st} = 1$ mm)	0.2042	0.1987	0.3042	0.1581	0.1542	0.2164
2 ($\delta_0 = 0.1$ mm)	0.1049	0.0993	0.3042	0.0585	0.0784	0.2164
2 ($\delta_0 = 1$ mm)	0.0	0.0	0.3042	0.0	0.0	0.2164

[a]Stitch failure.

Table 6 Shear buckling coefficients of isotropic and specially orthotropic square plates for different radii of one center delamination, r_d

r_d/a	k_0	γ_0
1/8	10.1333	316.34
1/4	9.9666	314.26
3/8	9.6972	311.50
1/2	9.4557	309.66

IV. Conclusions

The presented method determines the deformations and stability characteristics of the orthotropic stitched plate system with delaminations under axial compressive normal and shear loads and internal HTPs. This model is the first for such a complicated FRP stitched composite structure with delaminations under various combined loading configurations. The system currently has two plate layers but will be extended to several layers to form multi-layered plate model.

Compared to recent finite element methods, this method can give deformed configurations to obtain the system's behavior for given loading configuration in much shorter time. The presented model is also capable of determining the optimum locations for stitches, depending on delamination sizes and locations, to have a safer system against buckling.

The cohesive zone between laminates has been analyzed with finite element methods with huge calculation times recently. In this study, the zone is handled with a continuous mechanical spring model of the interlaminar adhesive layer, which presents the cohesive zone because springs can be broken if stresses exceed the limits. To be more realistic model, stitches are taken as discrete bilinear normal springs by considering initial imperfections. (Stitches are initially slack.) The stitch failure criterion is modeled as exceedance of the strain limit and will be modeled with Weibull distribution.

Various shapes of delaminations can be introduced to the system. In particular, elliptic shapes are more realistic and can be used to investigate cracks in the adhesive layer. Small rectangular shapes can be used for a time-dependent failure analysis of the system.

Consequently, it is shown that the presented model is very useful to determine the stability and design characteristics of a very complicated advanced FRP composite structure because one can predict how the system under consideration will function without spending too much time for calculations with finite element solvers and too much money to build prototypes of expensive FRP composites.

Acknowledgment

This work has been funded through NASA Cooperative Agreement NCC3-994, the "Institute for Future Space Transport" University Institute.

References

[1]Abrate, S., *Impact on Composite Structures*, Cambridge Univ. Press, Cambridge, England, U.K., 1998.

[2]Dransfield, K., Baillie, C., and Mai, Y., "Improving the Delamination Resistance of CFRP by Stitching—A Review," *Composites Science and Technology*, Vol. 50, No. 3, 1994, pp. 305–317.

[3]Adanur, S., Tsao, Y. P., and Tam, C. W., "Improving Fracture Resistance of Laminar Textile Composites by Third Direction Reinforcement," *Composites Engineering*, Vol. 5, No. 9, 1995, pp. 1149–1158.

[4]Lau, K., Ling, H., and Zhou, L., "Low Velocity Impact on Shape Memory Alloy Stitched Composite Plates," *Smart Materials and Structures*, Vol. 13, No. 2, 2004, pp. 364–370.

[5]Phoenix, S. L., Yavuz, A. K., Papoulia, K. D., and Hui, C. Y., "Buckling Analysis of Delaminated and Stitched Composite Plate System Under Hygro-thermal Pressure," *Journal of Engineering Materials and Technology*, Vol. 128, No. 1, 2006, pp. 117–122.

[6]Yavuz, A. K., and Kotil, T., "Free Vibrations of Rotating Adhesively Bonded Orthotropic Plates," *Mathematical and Computational Applications in Science and Engineering*, Vol. 1, No. 1, 1996, pp. 140–146.

[7]Yavuz, A. K., "Free Vibration Analysis of Rotating Adhesively Bonded Plates," Ph.D. Dissertation, Aeronautical Engineering Dept., Istanbul Technical Univ., Istanbul, Turkey, Feb. 1999.

[8]Whitney, J. M., *Structural Analysis of Laminated Anisotropic Plates*, Technomic, Lancaster, PA, 1987.

[9]Reddy, J. N., *Mechanics of Laminated Composite Plates: Theory and Analysis*, CRC Press, New York, 1997.

[10]Bulson, P. S., *The Stability of Flat Plates*, American Elsevier, New York, 1969.

B. Sankar
Associate Editor